Axial channeling of ultrarelativistic electrons

V. I. Telegin and M. Kh. Khokonov

Institute of Nuclear Physics Moscow State University

(Submitted 7 December 1981)
Zh. Eksp. Teor. Fiz. **83**, 260–274 (July 1982)

The dynamics of the motion of ultrarelativistic electrons in axial channeling is investigated. The analysis is based on solution of the kinetic equation recently obtained by Beloshitskiĭ and Kumakhov [Rad. Eff. Lett. **58**, 41 (1981) and Sov. Phys. JETP **55**, 265 (1982)]. The particle-dechanneling function was studied as a function of the type of crystal, particle energy, and entry angle into the crystal. It was found that for the greater part of the beam the principal mechanism of diffusion is scattering by electrons. It is shown that there is an optimal range of depths at which the fraction of channeled particles increases rapidly at the expense of quasichanneled particles. Here in a number of cases the dechanneling length for crystals with high atomic number can turn out to be greater than for light elements.

PACS numbers: 61.80.Mk

INTRODUCTION

Recently there has been a great increase in interest in study of the channeling of light relativistic particles, particularly electrons. This is due to the observation of the intense characteristic spontaneous radiation in channeling which was predicted by Kumakhov.[2] The spectral and angular characteristics of this radiation are greatly influenced by multiple scattering by electrons and by thermal vibrations of the nuclei. The multiple scattering of positive channeled particles has been studied in detail (see for example Refs. 3–6).

However, the nature of channeling of positive particles differs substantially from that of negative particles. This requires a new approach for discussion of the problem of multiple scattering of channeled particles. Such an approach was recently proposed in an article by Beloshitsky and Kumakhov,[1] in which a kinetic equation of the Fokker-Planck type was obtained for negative particles.

Axially channeled electrons move along trajectories of a rosette type.[7] Here the electron moves around an atomic string and is in a bound state. If the potential of the string is considered to be axially symmetric, the motion in its field will be characterized by two independent integrals of motion—the transverse energy and the angular momentum of the particle with respect to the axis. Therefore in this case it becomes necessary to discuss diffusion in two-dimensional phase space in the transverse energies and the angular momenta.[1] The kinetic equation obtained in this case has been solved numerically by computer with inclusion of the multiple scattering of channeled particles by electrons and nuclei of the crystal lattice.

For the energy range 1–10 GeV considered, a classical discussion of the motion of the electrons in the channel is applicable, since the number of levels of the transverse energy is quite large: $\nu\sim\gamma$ ($\gamma=1/(1-v^2/c^2)^{1/2}$ is the Lorentz factor). As the potential of the atomic axis we took the model potential $U(r)\sim r^{-1}$, where r is the distance to the string. In view of its simplicity, such a potential permits comparatively easy study of the main regularities and features of the axial channeling of negative particles. In the framework of this potential we have discussed the possibility of transition of electrons from the quasichanneling mode into an axial channel. The effect of atomic planes was not taken into account here.

1. THE POTENTIAL OF AN ATOMIC STRING FOR AXIAL CHANNELING OF ELECTRONS

Most theories of channeling are based on introduction of continuous potentials of atomic strings and planes.[8] For an electron at a distance r from an atomic string, with use of the Moliere screening function the following expression is obtained for the potential[9]:

$$U^n(r)=-\frac{2Ze^2}{d}\exp\left[-\frac{1}{2}\left(\frac{r}{u_\perp}\right)^2\right]\sum_{i=1}^{3}\alpha_i\int_0^\infty K_0\left(\beta_i\frac{u_\perp}{a_F}s\right)I_0\left(\frac{r}{u_\perp}s\right)\times\exp\left(-\frac{s^2}{2}\right)sds. \quad (1.1)$$

Here Ze is the charge of the nucleus, d is the distance between atoms in a string, and $\alpha_i=0.1$, 0.55, and 0.35; $\beta_i=6.0$, 1.2, and 0.3; $a_F=0.8853a_BZ^{-1/3}$, a_B is the Bohr radius, K_0 and I_0 are modified Bessel functions, and $u_\perp$ is the amplitude of the thermal vibrations of the atoms. The potential at a point r is defined as the sum of the potentials of all strings forming the crystal:

$$U(\mathbf{r})=\sum_n U^n(|\mathbf{r}-\mathbf{r}_n|). \quad (1.2)$$

Certain features of the axial channeling of negative particles permit the above expression to be replaced by a simpler one. In contrast to the channeling of positive particles, the potential well for electrons is significantly narrower. For positrons the region of distance to the string $r>a_F$ is most important, while the greatest effect on the behavior of electrons in channeling is from the region $r\sim a_F$. For such distances from the string Lindhard proposed a potential of the form $U(r)=\alpha/r$. In our calculations the potential of an atomic string was taken in the form

$$U(r)=-\alpha/r+U_0, \quad (1.3)$$

where $\alpha=\frac{3}{2}Ze^2a_F/d$. Introduction of the quantity U_0 is due to the necessity of cutting off the potential as a consequence of the influence of neighboring strings: $U_0=\alpha/r_0$, where $r_0=1/(\pi Nd)^{1/2}$ is the dimension of a channel and N is the number of atoms per unit volume

0038-5646/82/070142-09$04.00

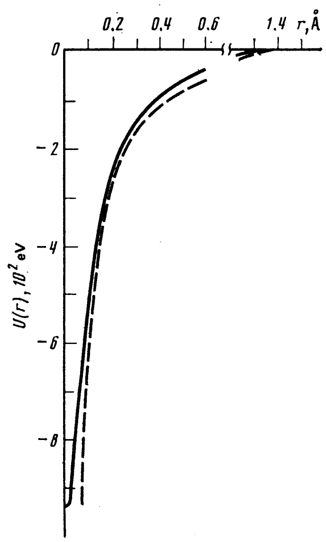

FIG. 1. Potential of an atomic string for tungsten ⟨111⟩ ($Z=74$). The solid curve is the potential calculated with Eq. (1.2), averaged over azimuthal angle. The dashed curve is the model potential (1.3).

in the crystal.

In Fig. 1 we have shown a comparison of the exact potential (1.2) averaged over the azimuthal angle, with expression (1.3) for the ⟨111⟩ direction in tungsten at temperature 20 ℃. In the calculation with Eq. (1.2) it was assumed that the thermal vibrations of the atoms are isotropic and the amplitudes of the thermal vibrations are determined according to the Debye model.

The region of greatest potential gradient lies within the limits $r\sim 2a_F$. The potentials (1.2) and (1.3) are closest in just this region. As the depth of the potential well for the expression (1.3) one can take the value $U_{\min}=\alpha/u_\perp$.

In the absence of multiple scattering, the transverse motion of the electrons in the potential (1.3) consists of ellipses whose foci coincide with the axis of the channel. The minimum and maximum distances of the electron orbit from the string $r_{\min}$ and $r_{\max}$ are

$$r_{min}=a(1-\eta),\quad r_{max}=a(1+\eta),\quad a=\alpha/2(|E_\perp|+U_0),$$
$$\eta=(1-2(|E_\perp|+U_0)M^2c^2/\alpha^2E)^{1/2},\quad M=r_i\psi_i\sin\varphi_i, \tag{1.4}$$

where a is the large semiaxis of the ellipse, η is the eccentricity of the orbit, M is the projection of the angular momentum on the channel axis z, r_i and φ_i are the initial polar coordinates of the particle in the transverse plane, and $E_\perp$ is the transverse energy of the electron,

$$E_\perp=U(r_i)+E\psi_i^2/2, \tag{1.5}$$

which corresponds to an angle of entry of the electron into the crystal ψ_i.

The period of the transverse motion in the field (1.3) is

$$T=\frac{\pi\alpha}{c}\frac{E^{1/2}}{8(|E_\perp|+U_0)^3}, \tag{1.6}$$

where c is the velocity of light and E is the energy of the incident electron.

The longitudinal velocity v_z can be assumed constant: $v_z\approx c$. In the preceding formulas we have taken into account the fact that for the transverse motion of the electrons in a channel $v_\perp \ll c$ and relativistic effects reduce to the increase of mass of the particle.

2. THE KINETIC EQUATION

For sufficiently thick crystals one can speak of statistical equilibrium in the transverse plane.[8] Here the behavior of a beam of electrons under conditions of channeling is described by a distribution function which depends only on the integrals of the motion $E_\perp$ and M. This distribution function will satisfy a kinetic equation of the Fokker-Planck type. This equation was obtained by Beloshitsky and Kumakhov and has the form[1]

$$\frac{\partial F}{\partial z}=\frac{\partial}{\partial E_\perp}\left(D_{\varepsilon\varepsilon}T\frac{\partial}{\partial E_\perp}\frac{F}{T}\right)+\frac{\partial}{\partial E_\perp}\left(D_{\varepsilon\mu}T\frac{\partial}{\partial M}\frac{F}{T}\right)$$
$$+\frac{\partial}{\partial M}\left(D_{\mu\varepsilon}T\frac{\partial}{\partial E_\perp}\frac{F}{T}\right)+\frac{\partial}{\partial M}\left(D_{\mu\mu}T\frac{\partial}{\partial M}\frac{F}{T}\right), \tag{2.1}$$

where $F(E_\perp,M,z)$ is the distribution function of particles in the channel at a depth $z=ct$, t is the time of motion of the particle in the channel, and T is the period of its transverse motion. In Eq. (2.1) we have omitted terms taking into account the change of the total energy of the particle, which is completely justified for the beam energies considered.

The diffusion coefficients in Eq. (2.1) have the form

$$D_{\varepsilon\varepsilon}=\frac{1}{2}\left\langle\frac{\overline{\Delta E_\perp{}^2}}{\Delta z}\right\rangle,\quad D_{\mu\mu}=\frac{1}{2}\left\langle\frac{\overline{\Delta M^2}}{\Delta z}\right\rangle,\quad D_{\mu\varepsilon}=D_{\varepsilon\mu}=\frac{1}{2}\left\langle\frac{\overline{\Delta E_\perp\Delta M}}{\Delta z}\right\rangle. \tag{2.2}$$

All of these quantities are expressed in terms of the mean square multiple scattering angle $\overline{\Delta\theta^2}$ by the formulas

$$\overline{\Delta E_\perp}=E\overline{\Delta\theta^2}/2,\quad M=0,\quad \overline{\Delta E_\perp{}^2}=E[E_\perp-U(r)]\overline{\Delta\theta^2},$$
$$\overline{\Delta M^2}=p^2r^2\overline{\Delta\theta^2}/2,\quad \overline{\Delta M\Delta E_\perp}=EM\overline{\Delta\theta^2}/2. \tag{2.3}$$

In these formulas we have taken into account the relativistic relation between the total energy and momentum of the electron, $E=pc$. The angle brackets ⟨...⟩ in Eq. (2.2) denote averaging over the period of the transverse motion:

$$\langle x\rangle=(2m_0\gamma)^{1/2}T^{-1}\int_{r_{min}}^{r_{max}}x\left[E_\perp-U(r)-\frac{M^2}{2m_0\gamma r^2}\right]^{-1/2}dr, \tag{2.4}$$

where $r_{\min}$, $r_{\max}$, and T for the potential (1.3) are given by Eqs. (1.4) and (1.6).

3. REGIONS OF CHANNELING AND QUASICHANNELING

In order to solve the kinetic equation (2.1) it is necessary to determine the region of possible variations of the transverse energies $E_\perp$ and the angular momenta M, and also to specify the boundary conditions for the distribution function.

We shall consider electrons to be channeled which are in a bound state in the field of an atomic string. The transverse energy of such particles is negative in the case of channeling and as the result of diffusion may vary from $-U_{\min}$ to zero ($U_{\min}$ is the depth of the potential well for the expression (1.3), $U_{\min} \approx \alpha/u_\perp$). Here for particles with a given value of transverse energy the diffusion in the angular momenta can change the magnitude of the latter also in a limited interval. If U_{eff} is the effective potential energy of an electron with a given value of angular momentum M:

$$U_{eff}=U(r)+M^2/2m_0\gamma r^2,$$

then the region of variation of the angular momenta is determined by the condition $E_\perp \geqslant U_{\text{eff}}^{\min}$, where $U_{\text{eff}}^{\min}$ is the minimum of U_{eff} for electrons with a given M. For the potential (1.3) the region of the solution of the Fokker-Planck equation is determined by the inequalities

$$-U_{min}\leqslant E_\perp\leqslant 0, \quad 0\leqslant M\leqslant\left[\frac{E}{2(|E_\perp|+U_0)}\right]^{1/2}\frac{\alpha}{c}. \tag{3.1}$$

Multiple scattering by the electrons of the crystal and by the thermal vibrations of the lattice lead to an increase of the transverse energy of a particle up to zero and to its escape from a bound state (i.e., from the channel). Here the particles go over to the quasi-channeling mode. If we divert our attention from the effect of atomic planes on such electrons and the possibility of their capture into a planar channel, we can assume that in the quasichanneling region an electron is in the field of a disordered system of atomic strings. Then the behavior of the particles in this case can be described by a distribution function which depends only on the transverse energy and which satisfies a one-dimensional diffusion equation of the Fokker-Planck type:

$$\frac{\partial F^{\text{II}}}{\partial z}=\frac{\partial}{\partial E_\perp}\left(D_{\varepsilon\varepsilon}{}^{\text{II}}\frac{\partial F^{\text{II}}}{\partial E_\perp}\right). \tag{3.2}$$

Here the superscript II indicates that the quantities considered are associated with the quasichanneling region.

The channeling region I and the quasichanneling region II for tungsten ⟨111⟩ at $E = 1$ GeV for the potential (1.3) are shown below in Fig. 7, where we have used the dimensionless variables

$$\varepsilon=dE_\perp/Ze^2, \quad \mu=cM/a_FE\psi^c, \tag{3.3}$$

and $\psi^c = (4Ze^2/dE)^{1/2}$ is the Lindhard critical angle. The curved portion *abc* is defined by the second inequality of (3.1).

The boundary conditions for Eq. (2.1) are such that there is no diffusion flux through the region bounded by the inequalities (3.1) (except the boundary $\varepsilon = 0$ between regions I and II). At the boundary $\varepsilon = 0$ it is necessary to join the solutions of Eqs. (2.1) and (3.2) in such a way as to provide continuity of the diffusion flow (details can be found in the Appendix).

4. DIFFUSION COEFFICIENTS

The solution of the kinetic equations (2.1) and (3.2) is based primarily on a knowledge of the diffusion coefficients, which are expressed in terms of the mean square multiple scattering angle. In an ideal crystal the increment of the transverse energy will be due to scattering by thermal vibrations of the nuclei and electrons of the crystal, i.e.,

$$\overline{\Delta\theta^2}/\Delta z=(\overline{\Delta\theta^2}/\Delta z)_{th}+(\overline{\Delta\theta^2}/\Delta z)_e.$$

The change of the transverse energy in multiple scattering by the electrons of the crystal can be expressed in terms of the total ionization loss of the channeled particle. At high energies, assuming that in close collisions the energy loss is proportional to the electron density in the channel, we can use the expression

$$\overline{\Delta E_\perp}=\frac{E\overline{\theta^2}}{2}=\frac{2\pi e^4NZL_e}{m_0\gamma v^2}n(r)\Delta z, \tag{4.1}$$

where $n(r)$ gives the behavior of the electron density in the channel as a function of the distance to the atomic string and L_e is the Coulomb logarithm.

If $U(r)$ is the potential of an atomic string, then the electron density in the channel can be determined from the Poisson equation

$$n(r)=\frac{1}{4\pi er}\frac{d}{dr}\left(r\frac{dU}{dr}\right).$$

We used the electron density calculated on the basis of the standard Lindhard potential[8]:

$$n(r)=3(r_0/a_F)^2(3+r^2/a_F^2)^{-2}, \tag{4.2}$$

where r_0 is the radius of the channel.

The necessity of taking into account scattering by thermal vibrations of nuclei in channeling of negative particles is due to the fact that they come close to the atomic string. Kitagawa and Ohtsuki[10] proposed a nuclear diffusion coefficient for nonrelativistic protons obtained from the corresponding expression for an unoriented target, multiplied by a Gaussian distribution of the nuclei in their thermal vibrations. In our case it is necessary to take into account only the relativistic increase of the particle mass. Then for the increment of the transverse energy of a channeled particle as a consequence of scattering by the thermal vibrations we have the formula

$$\frac{\overline{\Delta E_\perp}}{\Delta z}=\left(\frac{\overline{\Delta E_\perp}}{\Delta z}\right)_{\text{am}}P(r), \quad \left(\frac{\overline{\Delta E_\perp}}{\Delta z}\right)_{\text{am}}=\frac{E}{2L_{\text{rad}}}\left(\frac{21}{E\,[\text{MeV}]}\right)^2, \tag{4.3}$$
$$P(r)=(r_0/u_\perp)^2\exp(-r^2/u_\perp^2),$$

where $(\overline{\Delta E_\perp}/\Delta z)_{\text{am}}$ is the increment of the transverse energy in multiple scattering in an amorphous medium, L_{rad} is the radiation length, and $P(r)$ is the distribution of atoms in their thermal vibrations in the transverse plane.

In channeling of negative particles, the scattering of the greater number of them occurs on the electrons of the crystal. The value of the corresponding diffusion coefficient, as can be seen from Eq. (4.1), is determined by the charge of the target nuclei and by the behavior of the electron density in the channel, and in a number of cases the latter factor is the more important. For example, as a consequence of the more rapid falloff of the electron density with increase of the distance from the atomic axis, the electron diffusion coefficient in tungsten ⟨111⟩ is less in absolute value than in silicon ⟨111⟩ (see Fig. 2) in a large part of the channel, in spite of the higher atomic weight.

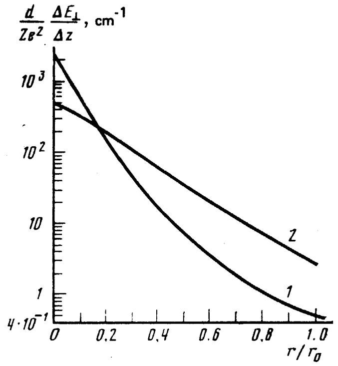

FIG. 2. Electronic diffusion coefficient ($\Delta E_\perp/\Delta z$) as a function of the distance to the atomic axis. 1—W ⟨111⟩ (r_0 = 1.36 Å), 2— Si ⟨111⟩ (r_0 = 1.16 Å). The energy of the incident electrons is 1 GeV.

At small distances from the axis $r \sim u_\perp$ the diffusion coefficient of scattering by thermal vibrations exceeds the electron diffusion coefficient by several orders of magnitude. For most crystals they are comparable at distances from the axis $r \sim 0.15 r_0$.

In the quasichanneling region the diffusion coefficient can be taken approximately the same as in an amorphous medium, although for positive values close to zero of the transverse energy, scattering by electrons will evidently be dominant. Then we have that the coefficient $D_{\varepsilon\varepsilon}{}^{\mathrm{II}}$ increases linearly with increase of the transverse energy:

$$D_{\varepsilon\varepsilon}{}^{\mathrm{II}}=(E_\perp+U_{min})\,(\Delta E_\perp/\Delta z)_{\mathrm{am}} \tag{4.4}$$

5. INITIAL DISTRIBUTION

If a unit electron flux $1/S_0$ hits the crystal (S_0 is the area per string), then the fraction of particles which pass through an area element of the transverse plane is

$$dN=S_0^{-1}r_{in}dr_{in}d\varphi_{in},$$

where r_{in} and φ_{in} are the initial polar coordinates of the electron. Converting this expression to the variables $E_\perp$ and M by means of the relations

$$E_\perp=U(r_{in})+E\psi_{in}{}^2/2, \qquad \varphi_{in}=a\sin(M/r_{in}p_\perp),$$

we have

$$dN=F_0(E_\perp, M)\,dE_\perp dM,$$

where $F_0(E_\perp, M)$ is the desired distribution normalized to the fraction of particles captured into the channeling mode for a given angle of entry into the crystal ψ_{in}:

$$F_0(E_\perp,M)=4r_{in}(p_\perp{}^2r_{in}{}^2-M^2)^{-1/2}\Big/S_0\left|\frac{dU}{dr}\right|_{r=r_{in}}; \tag{5.1}$$

here $p_\perp = p\psi_{\mathrm{in}}$, $S_0 = 1/Nd$, and N is the number of atoms per unit volume of the crystal.

As can be seen from Eq. (5.1), the initial distribution function is inversely proportional to the force acting on the particle at the point r_{in} of the channel, and also is determined by the initial angle of entry into the crystal. For the potential (1.3) the region in which the initial distribution (5.1) is given is determined by the inequality

$$0\leqslant M\leqslant c\psi_{in}r_{in}/E, \qquad r_{in}=\alpha(U_0+|E_\perp|+E\psi_{in}{}^2/2)^{-1}. \tag{5.2}$$

With normal incidence of the electron beam on the crystal, all electrons hitting the crystal have zero angular momenta with respect to the atomic string, i.e., their trajectories pass along the axis. As the entry angle into the channel is increased, states with higher angular momenta are filled as a whole.

For the potential (1.3) we have for the initial distribution function the expression

$$F_0(E_\perp, M) =(4r_{in}{}^3/S_0\alpha)\,(p_\perp{}^2r_{in}{}^2-M^2)^{-1/2}. \tag{5.3}$$

Integration of this expression over all possible values of the angular momenta and transverse energies corresponding to the channeling state gives the fraction of electrons captured into the channel for a given angle of entry into the crystal. We have

$$\Delta N_{\mathrm{chan}}=(1+E\psi_{in}{}^2/2U_0{}^2)^{-2}. \tag{5.4}$$

All of these particles have parameters of the elliptical orbits of the transverse motion such that their maximum departure from the axis does not exceed the dimensions of the channel, i.e., $r_{\max} \leqslant r_0$ ($r_{\max}$ is determined from Eq. (1.4)).

For normal incidence of the beam on the crystal all particles are captured into the region of negative values of the transverse energy (i.e., into a channel). However, they will undergo strong scattering by nuclei and rapidly leave the channel. For large ψ_{in} the fraction of particles captured into a channel is very small. Therefore there is some optimal region of angles ψ_{in} for which we should expect maximum capture of the electrons. Values of the optimal entry angles into the crystal can be found approximately by means of Eq. (5.3) if we assume that particles whose trajectories are such that $r_{\min} \leqslant u_\perp$ are not channeled ($r_{\min}$ is determined from Eq. (1.4)). In Fig. 3 we have shown the fraction of particles which enter a channel, calculated by this means (dashed line) and according to Eq. (5.4). It is evident that ΔN_{chan} depends strongly on the entry

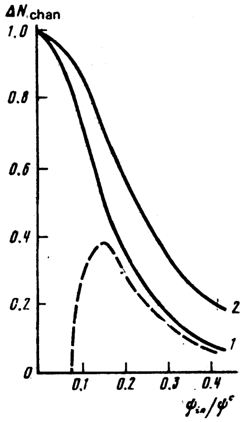

FIG. 3. Fraction of particles captured into axial channeling ΔN_{chan} as a function of the entry angle into the crystal ψ_{in}. 1—W⟨111⟩, 2—Si⟨111⟩. The dashed curve is the same for W⟨111⟩ on the assumption that in the initial distribution of electrons in the channel we have excluded particles whose transverse energies intersect a zone of radius $u_\perp$ near the atomic axis.

angle into the crystal. It follows from Fig. 3 that for tungsten ⟨111⟩ the optimal entry angles are $\psi_{\rm in}^{\rm opt} \approx 0.15\psi^c$. For most crystals the values of $\psi_{\rm in}^{\rm opt}$ lie in the range $\psi_{\rm in}^{\rm opt} \approx (0.1-0.3)\psi^c$. With increase of $\psi_{\rm in}$ the relative fraction of particles which enter the region of action of the nuclei decreases, as also can be seen from Fig. 3.

Obviously $1-\Delta N_{\rm chan}$ particles fall into the one-dimensional region with positive values of the transverse energy. The initial distribution in transverse energy for them is

$$F_0^{\rm II}(E_\perp)=2r_{in}^3/r_0^2\alpha,$$
$$r_{in}=\alpha(U_0-E_\perp+E\psi_{in}^2/2)^{-1}, \quad 0\leqslant E_\perp \leqslant E\psi_{in}^2/2. \tag{5.5}$$

This region of transverse energies corresponds both to particles whose orbit parameters are such that $r_{\rm max} > r_0$ and to particles with hyperbolic trajectories (the latter occur for entry angles $\psi_{\rm in} > (2U_0/E)^{1/2}$.

Analysis of the initial distribution (5.3) shows that the greater part of the electrons enter the channeling mode with transverse energies close to zero. For example, approximately 80% of the particles captured into a channel fall into the energy interval $-0.1U_{\rm min} \leqslant E_\perp \leqslant 0$ in tungsten ⟨111⟩ for an entry angle $\psi_{\rm min} = 0.15\psi^c$. For electrons with a given transverse energy, states with higher angular momenta are populated more densely. Thus, we should expect that in axial channeling electrons will be dechanneled mainly as the result of scattering by electrons, since the transverse trajectories of electrons with large angular momenta are far removed from the axis.

6. RESULTS OF NUMERICAL SOLUTION OF THE KINETIC EQUATION

Equations (2.1) and (3.2) were solved simultaneously by a numerical method (see the Appendix). The diffusion coefficients were taken in the form (2.2), (4.1), and (4.3). The initial condition was the distribution function (5.1). In the quasichanneling region the diffusion coefficient was taken in the form (4.4) as in a disordered system.

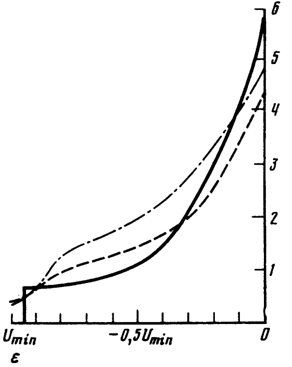

FIG. 4. Evolution of the distribution function (6.1) with depth of penetration of electrons with energy 1 GeV in Si ⟨111⟩ for an initial entry anlge $\psi_{\rm in}=0.15\psi^c$. The solid curve is the initial distribution. The dot-dash and dashed curves correspond to depths $z=5$ and 50 μm. The calculations were carried out without taking into account the initial distribution in the region of quasichanneling, i.e., on the assumption that all particles of the initial beam are captured into the channel.

In Fig. 4 we have shown the evolution of the distribution function with the depth of penetration of an electron beam with energy 1 GeV in a silicon crystal in the ⟨111⟩ direction. For convenience we have shown the distribution function as a function of the transverse energy, i.e., averaged over all angular momenta. The initial distribution in the region of positive values of the transverse energy was assumed to be zero, while in the channeling region it was normalized to unity, which corresponds to the assumption of 100 percent capture into a bound state of the initial beam.

The solution of the kinetic equation shows that electrons with transverse energies close to zero are dechanneled most rapidly (not considering, of course, electrons with $|E_\perp| \sim U_{\rm min}$, the fraction of which is very small). The number of particles

$$\Delta N=\int d\varepsilon F(\varepsilon,z), \quad F(\varepsilon,z)=\frac{2\alpha E\psi^c}{3c}\int dMF(E_\perp,M,z), \tag{6.1}$$

with $|E_\perp| \sim 0.5U_{\rm min}$, i.e., in the middle of the well, on the contrary, increases in comparison with their initial number by about a factor of five at a depth ~7.5 μm (in the ⟨111⟩ direction in silicon at an energy 1 GeV), and then begins to drop slowly. For example, in silicon (Fig. 4) the initial distribution of electrons is such that of all particles which enter the crystal (for an angle $\psi_{\rm in} = 0.15\psi^c$ about 70% of the initial beam is captured into the channeling mode) 10% are in the region of transverse energies $-U_{\rm min} \leqslant E_\perp \leqslant -0.2U_{\rm min}$. At a depth 5 μm already 14% of the initial beam is in this same energy interval, in spite of the fact that the total number of particles in the channel has decreased. At greater depths, as the solution shows, the distribution function changes with depth approximately in such a way that the fraction of particles in the energy interval $-U_{\rm min} \leqslant E_\perp \leqslant -0.2U_{\rm min}$ amounts to about a fourth of the total number of electrons remaining in the channel at this depth, and subsequently this ratio is almost unchanged with depth.

7. CALCULATION OF THE DECHANNELING FUNCTION

Practical interest is presented by a knowledge of the dechanneling function, i.e., the fraction of particles which remain in a given channel at a given depth. If $F(\varepsilon, \mu, z)$ is the distribution function of the particles in the channel, we shall be interested in the quantity

$$F(z)=\int_{-U_{min}}^{0} d\varepsilon \int_{0}^{\mu(\varepsilon)} d\mu F(\varepsilon,\mu,z). \tag{7.1}$$

Here $\mu(\varepsilon)$ is the curve which limits the solution of the problem in the direction of large values of angular momentum in accordance with Eq. (3.1).

In Fig. 5 we show the results of calculation of $F(z)$ for various crystals and at various energies. As in the preceding section, in these calculations we assumed for convenience that in the quasichanneling region the initial distribution is zero. However, in the region $\varepsilon < 0$ it has been normalized to unity. This choice of initial conditions corresponds to the assumption that all par-

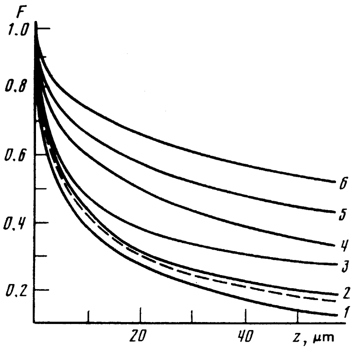

FIG. 5. Fraction of particles $F(z)$ [see Eq. (7.1)] remaining in a channel, as a function of depth. Curves 1, 2, and 3 correspond to the crystals Ge⟨111⟩, Si ⟨111⟩, and W ⟨111⟩ for an entry angle into the channel $\psi_{\text{in}}=0.15\psi^c$ and an initial beam energy 1 GeV. The dashed curve corresponds to Si ⟨111⟩ for $\psi_{\text{in}}=0.5\psi^c$ for the same energy. Curves 4, 5, and 6 correspond to energies 3, 5, and 7 GeV for Si ⟨111⟩ at $\psi_{\text{in}}=0.15\psi^c$. The calculations were carried out on the assumption that all particles of the initial beam are captured into the channel.

ticles of the initial beam are captured into the channeling regime, and that the further evolution of the beam is given by the solution of the kinetic equation.

In the simultaneous computer solution of Eqs. (2.1) and (3.2) the quasichanneling region was limited to the interval $0 \leqslant \varepsilon \leqslant \varepsilon_{\max} = 3.5\varepsilon^c$, where ε^c is the Lindhard critical energy. The boundary condition at $\varepsilon = 3.5\varepsilon^c$ was chosen so that

$$\frac{\partial}{\partial \varepsilon} F^{\text{II}}(\varepsilon, z)\,|_{\varepsilon=\varepsilon_{\max}} = 0. \tag{7.2}$$

This boundary condition limits the depths to which it is possible to solve the problem numerically with the chosen value of $\varepsilon_{\max}$. For $\varepsilon_{\max} = 3.5\varepsilon^c$ this depth is ~ 60 μm. At greater depths the influence of the limit begins to have a strong effect, and for the condition (7.2) the solution approaches a stationary value, which is clearly incorrect. The criterion of correctness of the solutions $F(\varepsilon, \mu, z)$ and $F^{\text{II}}(\varepsilon, z)$ obtained for a given value z is the inequality $F^{\text{II}}(0, z) \gg F^{\text{II}}(\varepsilon_{\max}, z)$.

In Fig. 5 we have shown the results of calculation of $F(z)$ in various crystals (silicon ⟨111⟩, tungsten ⟨111⟩, and germanium ⟨111⟩) for the same angle of entry into the channel $\psi_{\text{in}} = 0.15\psi^c$ and for the same electron energy $E = 1$ GeV. The value of $F(z)$ decreases to half at depths of 10, 7.5, and 6 μm respectively in tungsten, silicon, and germanium. $F(z)$ falls to 30% in the same crystals at respective depths 45, 23, and 18 μm. As can be seen, with increase of the depth the rate of dechanneling decreases.

For tungsten, as follows from the preceding discussion, the dechanneling depths were found to be greater than in silicon, in spite of the higher atomic number. This, generally speaking, is not in any way an obvious result. As we mentioned above, the electronic diffusion coefficient near the atomic axis in tungsten is several times greater in magnitude than in silicon. In addition, the initial distribution functions in these crystals are such that in silicon the states with larger absolute values of transverse energy are more densely populated, whereas the depths of dechanneling for such electrons are greater than for electrons with transverse energies close to zero. However, the basic fact here turned out to be that, as a consequence of the more rapid drop of the electron density with increase of the distance from the axis, in the principal part of the channel the average value of the diffusion coefficient for tungsten ⟨111⟩ is less than in the corresponding channel of silicon. In addition, the depth of the well itself in tungsten is greater than in silicon.

The fact that in heavy crystals with a high atomic number Z the dechanneling length is large has an important significance, since the intensity of spontaneous radiation in channeling predicted by Kumakhov[2] is proportional to $Z^2\chi_{1/2}$, where $\chi_{1/2}$ is the dechanneling length.

It is of interest to investigate the dependence of the dechanneling function on the energy of the incident beam. In Fig. 5 we have shown values of the dechanneling function $F(z)$ for silicon ⟨111⟩ for various energies of the incident electrons for the same angles of entry into the channel. As can be seen from the figure the depth $\chi_{1/2}$ at which the number of particles in the channel decreases to 1/2 increases with increase of the energy of the incident beam approximately according to a linear law, i.e., $\chi_{1/2} \sim \gamma$. We note that the diffusion coefficient is inversely proportional to the energy.

8. CALCULATIONS WITH THE INITIAL DISTRIBUTION IN THE QUASICHANNELING REGION

In the preceding paragraphs we have given the results of solution of the kinetic equation on the assumption that all particles from the initial beam are captured into the channeling regime and have negative values of the transverse energy. Such calculations provide the possibility of obtaining an idea of the nature of the variation of the distribution of electrons in transverse energy and angular momentum in a channel, and also of finding the dechanneling function. However, it is necessary to take into account also the fact that only a part of the initial beam is captured into the channel. The remaining electrons enter the region with positive transverse energy. The fraction of such particles is $1 - \Delta N_{\text{chan}}$, where ΔN_{chan} is determined by the expression (5.4).

Multiple scattering of particles by atomic strings in the quasichanneling region can lead to the result that part of them fall into the region with $\varepsilon < 0$, i.e., are captured into the channel. On the assumption that the region $\varepsilon > 0$ is a system of randomly located atomic strings, we can consider that the initial distribution of electrons in angular momentum in this region is uniform, and the distribution in transverse energy is given by Eq. (5.5).

The results of solution of the kinetic equation with allowance for the factors mentioned above are shown in Fig. 6, where we have drawn the dependence of the fraction of particles in the channel $F(z)$ on the depth for various angles of entry into the crystal. As the calculations show, a quite significant number of electrons

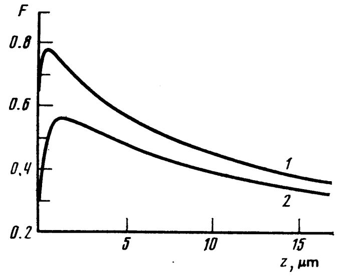

FIG. 6. Dechanneling functions $F(z)$ for Si⟨111⟩ at energy 1 GeV for various entry angles into the channel: 1—$\psi_{in}=0.2\psi^c$; 2—$\psi_{in}=0.35\psi^c$.

transfer from the quasichanneling region to a bound state as the result of multiple scattering, i.e., they go into the channel (see Fig. 6). For example, in silicon ⟨111⟩ for an entry angle $\psi_{in}=0.2\psi^c$ the number of particles in the channeling mode increases in comparison with the initial distribution by about 20%, and for an angle $\psi_{in}=0.35\psi^c$ it increases by 30%. As can be seen from Fig. 6, this redistribution of electrons occurs at very small depths ~1 μm.

9. CONCLUSIONS

The picture of the axial channeling of negative particles is the following. On incidence of the electron beam onto the crystal at sufficiently small angles to one of the crystallographic directions there is the possibility of capture of part of the electrons into a bound state in the field of the atomic strings. Such electrons have negative values of the transverse energy and are considered captured into the channeling regime. The interaction of an individual electron with an atomic string can be considered as having axial symmetry and can be approximated by a Coulomb potential. The transverse motion of the particles in such a field is characterized by two independent integrals of motion—the transverse energy and the angular momentum with respect to the axis, and consists of ellipses with foci which coincide with the atomic string.

The fraction of electrons captured into a channel is determined by the angle of entry into the channel. For various crystals the number of particles captured into a bound state is greater, the smaller is the area per string forming the channel and the more weakly it is screened by the electrons of the crystal (i.e., it depends on the ratio r_0/a_F).

Particles which have entered a channel have a distribution in phase space such that states with transverse energies close to zero are more densely populated. For a given transverse energy most particles come into the region of higher angular momenta (we note, however, that the initial distribution function in angular momentum is

$$F_0(\mu)=\int F_0(\varepsilon,\mu)\,d\varepsilon\sim(\mu_{max}^2-\mu^2)^{1/2},$$

i.e., on the whole the fraction of particles with higher angular momenta in the channel is smaller). With increase of the entry angle the number of particles captured into a channel decreases rapidly, and in return the relative fraction of particles with larger absolute values of the transverse energy increases. If we compare the fraction of particles which have transverse energies in the interval $0\leqslant|E_\perp|\leqslant 0.1U_{min}$ in relation to the total number of particles which have entered the channel, then for example in germanium ⟨111⟩ for entry angles $0.1\psi^c$ and $0.3\psi^c$ it amounts to respectively 75 and 60%.

Particles captured into the channeling regime undergo multiple scattering by electrons of the crystal and the thermal vibrations of the nuclei of the lattice. The existence of two integrals of motion leads to the result that it is necessary to consider diffusion in the two-dimensional space of transverse energy and angular momentum. The particle distribution in the channel satisfies the Fokker-Planck kinetic equation. Analysis of the diffusion coefficients in this equation shows that near an atomic string, $r\leqslant u_\perp$, there is a strong dominance of scattering by nuclei, the contribution of which is comparable with scattering by electrons at distances from the axis $r\approx 0.15r_0$. Thus, in the greater portion of the channel, electron scattering is dominant. The diffusion coefficients averaged over the period of oscillations in the channel are such that diffusion in the transverse energy dominates over diffusion in angular momentum. For transverse energies of greater absolute value the influence of the latter factor is negligible, but in the principal region (ε close to zero) the two factors are comparable.

At small angles of entry into the channel $\psi_{in}\lesssim 0.1\psi^c$ for most crystals, scattering by nuclei will evidently dominate in view of the fact that most electrons captured into a channel have small impact parameters. This should lead to rapid dechanneling at small depths. The optimum entry angles lie in the range $\psi_{in}\sim(0.1-0.3)\psi^c$.

The quasichanneling region can be represented in the first approximation as a system of randomly located strings. The evolution of the electron distribution in transverse energy in this region is described by a one-dimensional kinetic equation. Multiple scattering of electrons by atomic strings in such a system leads to the result that a part of them are captured into a bound state. Therefore at small depths ~1 μm the total number of particles in a channel increases appreciably in comparison with the initial number (see Fig. 6). Then the number of electrons with transverse energies close to zero ($0\leqslant|E_\perp|\leqslant 0.1U_{min}$) begins to decrease rapidly, whereas in the center of the potential well, on the other hand, it continues to increase, up to depths of ~2–3 μm.

Decrease of the dechanneling depth with increase of the entry angle into the crystal occurs first of all because of the decrease of the fraction of particles initially captured into the channel. It is an interesting fact, however, that calculations on the assumption of capture of all electrons of the initial beam into a channel also give a decrease of the dechanneling depth with increase of the entry angle (see Fig. 5, dashed line). If we take into account that the increase of the entry angle leads to an increase of the fraction of electrons with large absolute values of transverse energy (relative to all particles captured in the channel), then it would appear that the reverse situation should occur, since electrons with transverse energies close to zero are dechanneled more rapidly. These results are explained by the already noted redistribution of the electrons in transverse energy space at small depths (increase of the number of particles in the center of the potential well), when the total number of particles in the channel still does not change appreciably.

The fact that for tungsten ⟨111⟩ ($Z=74$) the dechanneling depths were found to be greater than, for example, in silicon ⟨111⟩ ($Z=14$) also is not at all obvious and is apparently due to the more rapid drop in the electron density in the channel and to the significantly greater depth of the potential well (about nine times). Thus, in axial channeling of electrons as a whole electron scattering is dominant. A characteristic feature in the dependence of the number of particles remaining in the channel on the depth is initially a rapid drop at comparatively small depths and a significantly slower drop at greater depths. On increase of the energy of the incident electrons the depth values at which the number of particles in the channel decreases by a factor of two grow approximately in proportion to the energy: $\chi_{1/2} \sim E$.

APPENDIX

Numerical solution of the kinetic equation of particle balance

The kinetic equations which describe the diffusion in the depth z of the particle distribution were solved in the region of variation of the generalized coordinates ε and μ with the curved part of the boundary abc shown in Fig. 7. Region I corresponds to the parameters of channeled particles. In this region the distribution functions satisfy the equation

$$\frac{\partial F}{\partial z}=\frac{\partial}{\partial \varepsilon}\left(TD_{11}\frac{\partial}{\partial \varepsilon}\frac{F}{T}\right)+\frac{\partial}{\partial \mu}\left(TD_{22}\frac{\partial}{\partial \mu}\frac{F}{T}\right)$$
$$+\frac{\partial}{\partial \varepsilon}\left(TD_{12}\frac{\partial}{\partial \mu}\frac{F}{T}\right)+\frac{\partial}{\partial \mu}\left(TD_{21}\frac{\partial}{\partial \varepsilon}\frac{F}{T}\right), \quad D_{12}=D_{21}. \tag{A1}$$

At the outer limit of this region, which is not common with region II, the normal component Γ_n of the diffusion flux is equal to zero:

$$\Gamma\mathbf{n}=\sum_{\alpha=1,2} T\left(D_{\alpha 1}\frac{\partial}{\partial \varepsilon}\frac{F}{T}+D_{\alpha 2}\frac{\partial}{\partial \mu}\frac{F}{T}\right)n_{\alpha}=0. \tag{A2}$$

Region II, which is bounded on the right by a sufficiently large value $\varepsilon_{\max}$, corresponds to the parameters of quasichanneled particles. In region II the distribution function satisfies an equation with a one-dimensional coordinate operator

$$\frac{\partial F}{\partial z}=\frac{\partial}{\partial \varepsilon}\left(D_{11}\frac{\partial F}{\partial \varepsilon}\right), \tag{A3}$$

in which D_{11} does not depend on μ. The problem which arises here of matching the component of the diffusion flux normal to the boundary between the regions I and II was solved in the calculations in the following way.

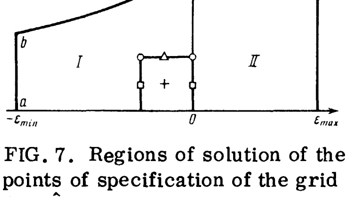

FIG. 7. Regions of solution of the difference equations and points of specification of the grid functions: + —F, T, D_{12}, Λ_3, $\hat{F}$; □—D_{11}, Δ—D_{22}, ○—intermediate points of calculation of $\Lambda_3 F$.

The solution of Eqs. (A1) and (A3) can be treated as the limit of a sequence of solutions $F^{(n)}$ of a single equation (A1) continued into region II, where in region II the diffusion coefficients $D_{22}^{(n)}$ and $D_{12}^{(n)}=D_{21}^{(n)}$ are small but nonzero and as $n\to\infty$ they approach zero. For reasons of physical causality one can assume that for fixed n the coordinate operator is uniformly elliptical, and the continuation to the entire boundary of the condition (A2) assures that it is self-adjoint. Then it is possible to write down formally a homogeneous conservative difference scheme[11] for Eq. (A1) over the entire region I and II. With this approach, continuity of the flux through the boundary between the region I and II is assured, including the case of discontinuous coefficients. At the same time it is not difficult to program an algorithm for calculation of the solution in which one explicitly excludes all operations which contain zero diffusion coefficients. For this purpose it is sufficient to organize the calculations individually in regions I and II.

The cell of the coordinate grid and the points for determination of the grid functions are shown arbitrarily in Fig. 7. In the calculations whose results we have discussed above, difference grids with 20 × 20 cells in region I and 140 × 20 in region II were used. We shall consider the difference operators

$$\Lambda_0 F=\Lambda_1 F+\Lambda_2 F=\left(TD_{11}\left(\frac{F}{T}\right)_{\varepsilon^+}\right)_{\varepsilon^-}+\left(TD_{22}\left(\frac{F}{T}\right)_{\mu^+}\right)_{\mu^-},$$
$$\Lambda_3 F=\left(TD_{12}\left(\frac{F}{T}\right)_{\mu_0}\right)_{\varepsilon_0}+\left(TD_{21}\left(\frac{F}{T}\right)_{\varepsilon_0}\right)_{\mu_0}, \tag{A4}$$

where the superscripts ± indicate right and left or respectively upper and lower difference derivatives. The mixed derivatives in Eq. (A4) were approximated by symmetric difference operators in a nine-point pattern.[12] In region I for solution of Eq. (A1) we used a partially factorized difference scheme[11]:

$$(I-h\sigma\Lambda_2)(I-h\sigma\Lambda_1)\hat{F}=F+h(1-\sigma)\Lambda_0 F$$
$$+0.5h\Lambda_3 F+0.5h\Lambda_3\hat{F}, \tag{A5}$$

where h is the step in the depth z and σ is the weighting factor for the operator Λ_0 in the next layer in z. The last term contains the desired values of the grid function $\hat{F}$ and therefore for solution of the difference equations (A5) we carried out several (usually three) iterations with the zeroth approximation of F in the preceding layer. Since in the problem considered the coefficient D_{12} is not small, it was desirable to decrease as much as possible all errors in approximation of terms with mixed derivatives for increase of the step in depth.

In region II $\Lambda_2=0$ and $\Lambda_3=0$, so that the scheme (A5) takes the form of the one-dimensional equations

$$(I-h\sigma\Lambda_1)\hat{F}=F+h(1-\sigma)\Lambda_1 F, \tag{A6}$$

which approximate Eq. (A3) and which were solved along the lines of the points $\mu=\text{const}$. At the points near the boundary of the regions $\varepsilon=0$, the equations (A5) were used for determination of the initial values of the adjustment coefficients for Eq. (A6) in terms of the coefficients calculated in region I.

The curved portion of the left boundary was fitted by a broken line with sections parallel to the ε and μ coordinate axes. The coordinates of the boundary cells were given by means of two arrays. The boundary condition (A2) was placed at the approximate boundary, since this has no substantial effect on processes inside regions I and II. Use of the condition (A2) at the right-hand boundary of region II permitted a check of the conservation of the total number of particles up to the establishment of the stationary distribution $F=\text{const}$. In the systematic calculations we chose the value $\sigma=0.65$ at which the grid function changes monotonically and, on the other hand, the total number of particles is satisfactorily preserved in the two regions. As a whole the difference scheme (A5) and (A6) has a second order of approximation in ε and μ and a first order in z.

[1] V. V. Beloshitsky and M. A. Kumakhov, Rad. Eff. Lett. **58**, 41 (1981). V. V. Beloshitskiĭ and M. A. Kumakhov, Zh. Eksp. Teor. Fiz. **82**, 462 (1982) [Sov. Phys. JETP **55**, 265 (1982)].

[2] M. A. Kumakhov, Dokl. Akad. Nauk SSSR **230**, 1077 (1976) [Sov. Phys. Doklady **21**, 581 (1976)].

[3] V. V. Beloshitskiĭ and M. A. Kumakhov, Zh. Eksp. Teor. Fiz. **62**, 1144 (1972) [Sov. Phys. JETP **35**, 605 (1972)].

[4] E. Bonderup, H. Esbensen, and J. U. Andersen, Rad. Eff. **13**, 9 (1972).

[5] V. A. Bazylev, V. V. Beloshitskiĭ, N. K. Shevago, M. A. Kumakhov, and Kh. Trikalinos, Zh. Eksp. Teor. Fiz. **80**, 608 (1981) [Sov. Phys. JETP **53**, 306 (1981)].

[6] V. V. Beloshitskiĭ and Kh. Trikalinos, Tesisy X Vsesoyuznoĭ konferentsii po primeneniyu luchkov zaryazhennykh chastits (Abstracts of the Tenth All-Union Conf. on Application of Charged-Particle Beams), Moscow State University, 1979, p. 35.

[7] H. J. Kreiner, F. Bell, R. Sizmann, D. Harder, and W. Hüttl, Phys. Lett. **A33**, 135 (1970).

[8] J. Lindhard, Influence of Crystal Lattice on Motion of Energetic Charged Particles, Mat.-Fys. Medd. Dan. Vid. Selsk. **34**, No. 14 (1965). Russ. transl., Usp. Fiz. Nauk **99**, 249 (1969).

[9] J. H. Barrett, Phys. Rev. **B3**, 1527 (1971).

[10] M. Kitagawa and Y. H. Ohtsuki, Phys. Rev. **B8**, 3117 (1973).

[11] A. A. Samarskiĭ, Vvedenie v teoriyu raznostnykh skhem (Introduction to the Theory of Difference Schemes), Moscow, Nauka, 1971, Chapter 3.

[12] A. A. Samarskiĭ and E. S. Nikolaev, Metody resheniya setochnykh uravneniĭ (Methods of Solution of Grid Equations), Moscow, Nauka, 1978, Chapter 5.

Translated by Clark S. Robinson